

# 6-D weak-strong beam-beam simulation study of proton lifetime in presence of head-on beam-beam compensation in the RHIC

Y. Luo,

August 2010

Collider Accelerator Department  
**Brookhaven National Laboratory**

**U.S. Department of Energy**

USDOE Office of Science (SC)

Notice: This technical note has been authored by employees of Brookhaven Science Associates, LLC under Contract No. DE-AC02-98CH10886 with the U.S. Department of Energy. The publisher by accepting the technical note for publication acknowledges that the United States Government retains a non-exclusive, paid-up, irrevocable, world-wide license to publish or reproduce the published form of this technical note, or allow others to do so, for United States Government purposes.

## **DISCLAIMER**

This report was prepared as an account of work sponsored by an agency of the United States Government. Neither the United States Government nor any agency thereof, nor any of their employees, nor any of their contractors, subcontractors, or their employees, makes any warranty, express or implied, or assumes any legal liability or responsibility for the accuracy, completeness, or any third party's use or the results of such use of any information, apparatus, product, or process disclosed, or represents that its use would not infringe privately owned rights. Reference herein to any specific commercial product, process, or service by trade name, trademark, manufacturer, or otherwise, does not necessarily constitute or imply its endorsement, recommendation, or favoring by the United States Government or any agency thereof or its contractors or subcontractors. The views and opinions of authors expressed herein do not necessarily state or reflect those of the United States Government or any agency thereof.

C-A/AP/#394  
August 2010

# **6-D weak-strong beam-beam simulation study of proton lifetime in presence of head-on beam-beam compensation in the RHIC**

Y. Luo, W. Fischer  
Brookhaven National Laboratory, Upton, NY 11973, USA



**Collider-Accelerator Department  
Brookhaven National Laboratory  
Upton, NY 11973**

Notice: This document has been authorized by employees of Brookhaven Science Associates, LLC under Contract No. DE-AC02-98CH10886 with the U.S. Department of Energy. The United States Government retains a non-exclusive, paid-up, irrevocable, world-wide license to publish or reproduce the published form of this document, or allow others to do so, for United States Government purposes.

# 6-D weak-strong beam-beam simulation study of proton lifetime in presence of head-on beam-beam compensation in the RHIC

Y.Luo, W. Fischer

Brookhaven National Laboratory, Upton, NY 11973, USA

In this note we summarize the calculated particle loss of a proton bunch in the presence of head-on beam-beam compensation in the Relativistic Heavy Ion Collider (RHIC). To compensate the head-on beam-beam effect in the RHIC 250 GeV polarized proton run, we are introducing a DC electron beam with the same transverse profile as the proton beam to collide with the proton beam. Such a device is called an electron lens (e-lens). In this note we first present the optics and beam parameters and the tracking setup. Then we calculate and compare the particle loss of a proton bunch with head-on beam-beam compensation, phase advance of  $k\pi$  between IP8 and the center of the e-lens and second order chromaticity correction. We scanned the proton beam's linear chromaticity, working point and bunch intensity. We also scanned the electron beam's intensity, transverse beam size. The effect of the electron-proton transverse offset in the e-lens was studied. In the study 6-D weak-strong beam-beam interaction model a la Hirata is used for proton collisions at IP6 and IP8. The e-lens is modeled as 8 slices. Each slice is modeled with as drift-( 4D beam-beam kick )-drift.

## 1 Optics and Beam Parameters

In the following simulation we adopt the Blue ring lattice for 250 GeV RHIC polarized proton run. Table 1 gives the optics and beam parameters for the proton beam for this study. Figure 1 shows the  $\beta$  function and horizontal dispersion along the ring. The proton beams collide at IP6 and IP8 where  $\beta^*$ s are 0.5 m.  $\beta^*$ s at all other non-colliding IPs are 10 m. The normalized rms transverse emittance  $\epsilon_n$  is 2.5 mm.mrad. The longitudinal beam area is 0.17 eV.s, which gives an rms beam momentum spread of  $0.14 \times 10^{-3}$  and an rms bunch length of 0.44 m.

To compensate the proton-proton beam-beam effect in the RHIC 250 GeV polarized proton run, especially to reduce the large tune shift and tune spread generated from the proton-proton beam-beam interactions at IP6 and IP8, we are introducing an DC electron beam with the same transverse profile as the proton beam to collide with the proton beam around IP10 [1, 2]. Such device to provide the electron beam is called electron lens (e-lens). Figure 2 shows the layout of RHIC head-on beam-beam compensation scheme. There will be two e-lenses for the head-on beam-beam compensation, one for the Blue and one for the Yellow rings. In the current design, the e-lenses are to be placed 1 m north in the Blue ring and 1 m south in the Yellow ring around IP10. The effective electron-proton interaction length is 2 m long.

So far the 250 GeV polarized proton run with  $\beta^* = 0.5$  m was not yet demonstrated. In the 2009 250 GeV RHIC polarized proton run, the  $\beta^*$ s at IP6 and IP8 were about 0.7 m. For the  $\beta^* = 0.5$  m lattice to be used in the study, the  $\beta^*$  at IP6 and IP8 from the lattice model are actually 0.53 m. The  $\beta$ s in the e-lens are 10 m. From Figure 1, there are about  $\pm 1.0$  m horizontal dispersion in the IR6 and IR8 which is different from the larger  $\beta^*$  lattices we have used in the previous proton run. The lattice with  $\beta^* = 0.5$  m to be used in this study may need further optimization [3].

For the above nominal lattice, with any beam-beam interaction, the horizontal and vertical betatron phase advances between IP6 and IP8 are  $(10.6\pi, 9.7\pi)$ . The phase advances between IP8 and the center of e-lens are  $(8.5\pi, 11.1\pi)$ . The phase advances between IP6 and the center of e-lens are  $(19.1\pi, 19.6\pi)$ . To better compensate the non-linear force from the proton-proton collision at IP8 with the e-lens around IP10, we will adjust the betatron phase advances between IP8 and the center of e-lens to be multiples of  $\pi$  in both the horizontal and vertical planes. After phase adjustment, the phase advances between IP8 and the center of e-lens will be  $(9.0\pi, 11.0\pi)$ .

The total linear beam-beam tune shift, or the total beam-beam parameter from proton-proton collisions

Table 1: Parameters for the proton beams

quantity	unit	value
<b>lattice</b>		
ring circumference	m	3833.8451
energy	GeV	250
relativistic $\gamma$	-	266
proton-proton collision points	-	IP6, IP8
location of e-lens	-	near IP10
$\beta_{x,y}^*$ at IP6 and IP8	m	0.53
$\beta_{x,y}^e$ at e-lens	m	10.0
$\beta_{x,y}^*$ at all other IPs	m	10.0
betatron phases between IP6 and IP8	(10.6 $\pi$ , 9.7 $\pi$ )	
betatron phases between IP6 and e-lens center	(8.5 $\pi$ , 11.1 $\pi$ )	
betatron phases between IP6 and e-lens center	(19.1 $\pi$ , 19.6 $\pi$ )	
<b>transverse parameters</b>		
normalized rms emittance $\epsilon_{x,y}$	mm·mrad	2.5
rms beam size at IP6 and IP8 $\sigma_{x,y}^*$	mm	0.068
rms beam size at e-lens $\sigma_{x,y}^e$	mm	0.31
tunes		(28.67, 29.68)
linear chromaticities		(1, 1)
second order chromaticities without correction		(2400, 2700)
proton-proton beam-beam parameter per IP		-0.01 * $N_p/(1.0 \times 10^{11})$
<b>longitudinal parameters</b>		
harmonic number	-	360
rf cavity voltage	kV	300
rms longitudinal bunch area	eV·s	0.17
rms momentum spread	-	$0.14 \times 10^{-3}$
rms bunch length	m	0.44

at IP6 and IP8 is

$$\xi_{pp} = -\frac{N_p r_p}{4\pi\epsilon_n} \times N_{IP}. \quad (1)$$

Here  $r_p$  is the classical proton radius. The number of proton-proton collision points  $N_{IP} = 2$ . In the following study we will focus on three bunch intensities,  $N_p = 2.0 \times 10^{11}$ ,  $2.5 \times 10^{11}$  and  $3.0 \times 10^{11}$ . From Eq. (1), the total proton-proton beam-beam parameters with 2 collision points are  $-0.020$ ,  $-0.024$ , and  $-0.030$ . There is not enough space in the current RHIC polarized proton tune space (2/3, 7/10) to hold all the beam-beam tune shift and tune spread generated by the proton-proton collisions with bunch intensity above  $2.0 \times 10^{11}$ . We define full and half head-on beam-beam compensations to compensate full or half total proton-proton beam-beam parameter. In the following study, we will mainly focus on the half beam-beam compensation. The full head-on beam-beam compensation introduces too much nonlinearities into the proton beam dynamic and therefore deteriorates the proton particle's dynamic aperture.

## 2 Tracking Setup

### 2.1 Beam-beam interaction modeling

Considering  $\beta^*$  is comparable to the bunch length at IP6 and IP8, the 6-D weak-strong synchro-beam map a la Hirata [4] is used to calculate the proton-proton beam-beam interactions. The e-lens will be split into 8 slices and for each slice, considering the electron beam is a DC beam, a drift-4D weak-strong beam-beam kick-drift modeling is used to calculate the kick the proton test particles receive from the electron beam. The 4D weak-strong beam-beam kick is based on the equations by Bassetti-Erskine [5]. The strong proton beam in another ring and the electron beam are considered rigid and will not be affected by the test particles in the simulation.

The particle motion in the magnetic elements is tracked with the 4th order symplectic integration by R. Ruth [6]. To save the time involved in the numeric tracking, we use thin multipoles in the lattice model. That

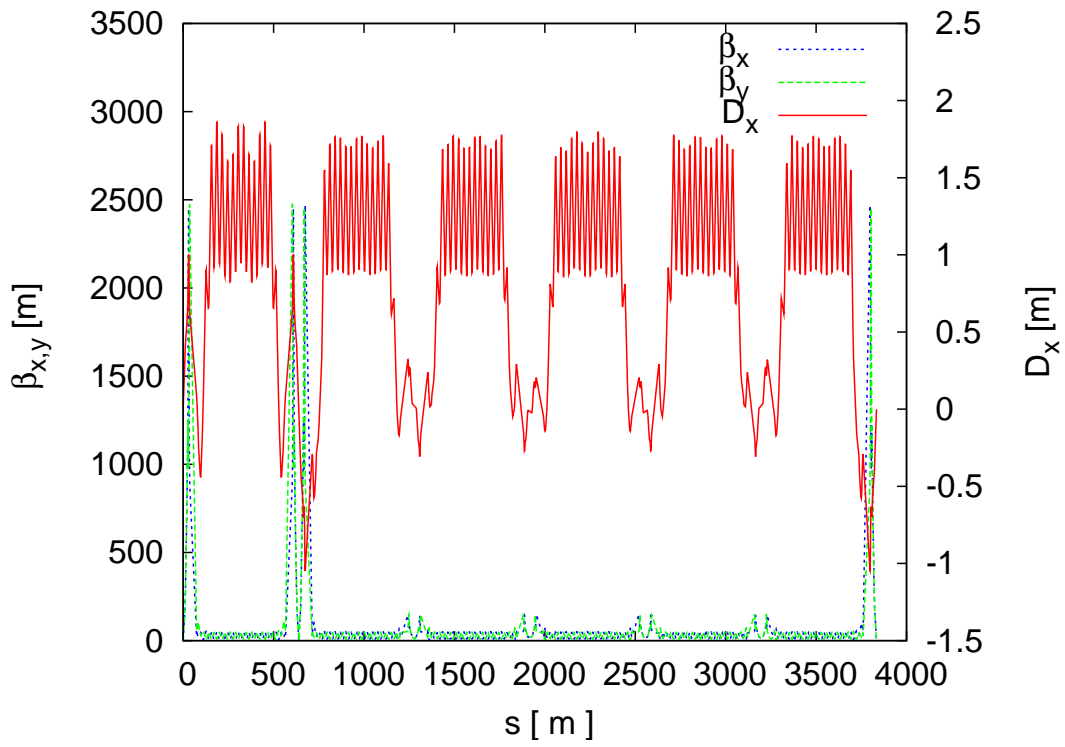


Figure 1: Layout of RHIC head-on beam-beam compensation.

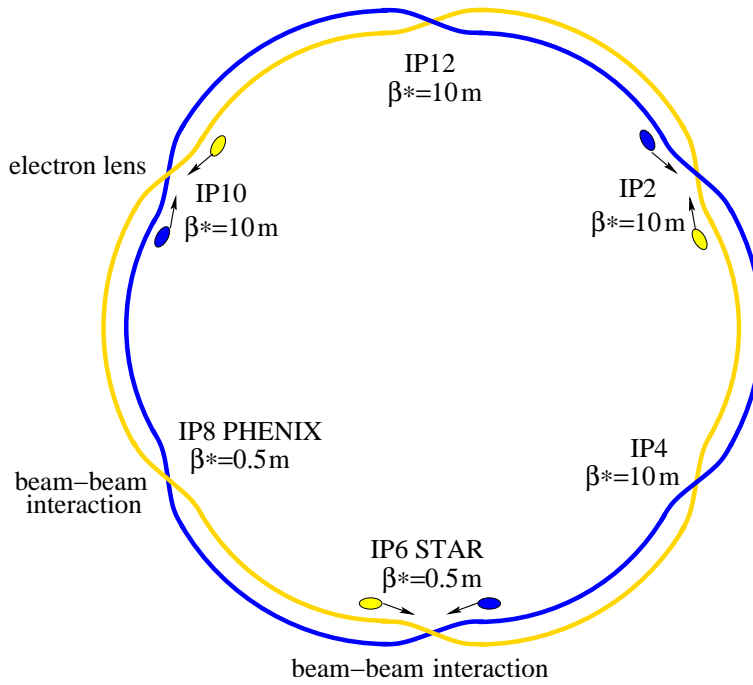


Figure 2: Lattice functions in the tracking model.

is, the non-zero length multipoles will be replaced by drift–multipole kick–drift. The tunes and chromaticities will be re-matched. In the study the tunes of zero amplitude particles are always set to (28.67, 29.68) and the linear chromaticities are set to (+1, +1) with beam-beam and compensations if included.

## 2.2 Limitation in lifetime tracking

To better reflect the particle loss in the real operation, we need a realistic lattice model. For the RHIC rings, the lattice model should include the correct linear optic model, all the non-linear magnetic field errors in the interaction regions and in the main dipoles and quadrupoles, and all the known electric and mechanic errors and noises. We know that the multipole field errors in the triplet quadrupoles and separation dipoles in the interaction regions play a crucial role in the reduction of the proton dynamic aperture. We also observed tune modulations and 10 Hz closed orbit oscillation of the beams. Currently a feedback is commissioned to correct the 10 Hz closed orbit oscillation. In the following study we only include the IR multipole field errors in the lattice.

Particle loss rate is well defined and measurable in the accelerator operation. In the simulation, limited by the computing time, we are able to track particles up to  $10^7$  turns which is equivalent to about 2 minutes in the real operation. The particle loss rate change in 2 minutes can be clearly monitored. However, to save computing time, most of the time we track the particles in a proton bunch up to  $2.0 \times 10^6$  turns which is equivalent to 24 seconds of real time.

Most particle lost are those with large transverse amplitude and large momentum deviation. However, for a Gaussian distribution of particles, there are few particles in the bunch tail. Therefore, to better represent the particles in the Gaussian bunch tail and to overcome the statistical error in the calculated particle loss rate, we need a large number of macro-particles and a good Gaussian distribution generator. In this study the Gaussian distribution generator provided in the Gnu Scientific Library (GSL) [7] is used.

## 2.3 Tracking with hollow Gaussian particle distribution

One solution is to track particles in a hollow Gaussian distribution of a proton bunch. This is based on the assumption that the particles in the bunch core are not lost in the tracking turns. To use this method, the boundary between the stable core and the unstable bunch tail needs to be carefully determined. We will first calculate the minimum dynamic apertures in several angles the x-y planes [8] and then set the boundary well below the minimum radial dynamic aperture. After tracking, we also need to check if there are particles lost on the edge of boundary. If there are particles lost on or close to the boundary, the particle loss rate is under-estimated and we need to set a lower boundary and re-do the tracking.

As an example, we first track 12800 particles of a 6-D Gaussian proton bunch up to  $2 \times 10^6$  turns. It turns out that there is only one of the 12800 macro-particles lost in  $2 \times 10^6$  turns. If we track 6400 particles in a hollow Gaussian bunch and their initial transverse amplitudes are above  $3\sigma$ , there will be 19 particles lost. 6400 macro-particles in the hollow Gaussian distribution represent a total of 105634 particles of a 6-D Gaussian proton bunch. Therefore, tracking with hollow Gaussian distribution saves computing time and also reduces the statistics errors in the particle loss rate calculation.

## 2.4 Generating a hollow Gaussian distribution

Here we go through the procedure to generate the initial particle coordinates of a hollow Gaussian distribution of a proton bunch. The initial normalized particle coordinates  $(x_n, p_{xn}, y_n, p_{yn}, z, \delta = dp/p_0)$  are generated with independent Gaussian distributions. The rms values of  $x_n$  and  $p_{xn}$  are  $\sqrt{\epsilon_x \beta_x}$ , the rms values of  $y_n$  and  $p_{yn}$  are  $\sqrt{\epsilon_y \beta_y}$ .  $\epsilon_x = \sqrt{\epsilon_{x,n}/\gamma}$  and  $\epsilon_y = \sqrt{\epsilon_{y,n}/\gamma}$  are the horizontal and vertical rms emittances.  $\beta_x$  and  $\beta_y$  are the horizontal and vertical  $\beta$  functions at the starting point of the tracking. In our study, the starting point is IP6. The rms bunch length is 0.44 m. The rms is momentum spread is  $0.14 \times 10^{-3}$ .

With the normalized coordinates, we then calculate the relative transverse amplitude  $N_t = \sqrt{N_x^2 + N_y^2}$  in the unit of transverse beam rms size.  $N_x$  and  $N_y$  are the amplitudes of particles in the horizontal and vertical planes,  $N_{x,y} = \sqrt{J_{x,y}/J_{rms,x,y}}$ , where  $J_{x,y}$  are the particle's horizontal and vertical action,  $J_{rms,x,y} = \epsilon_{x,y}/2$  are the rms action for the beam. Similarly we calculate the relative longitudinal amplitude  $N_l = \sqrt{N_z^2 + N_\delta^2}$  in unit of longitudinal phase space beam rms size, where  $N_z = z/\sigma_z$ ,  $N_\delta = \delta/\sigma_\delta$ .

In the sampling process, we only pick out these particles whose transverse amplitude  $N_t$  is larger than the pre-determined tracking transverse boundary or whose longitudinal amplitude  $N_l$  is larger than the pre-determined longitudinal boundary. Normally we track 4800 particles of a hollow Gaussian distribution.

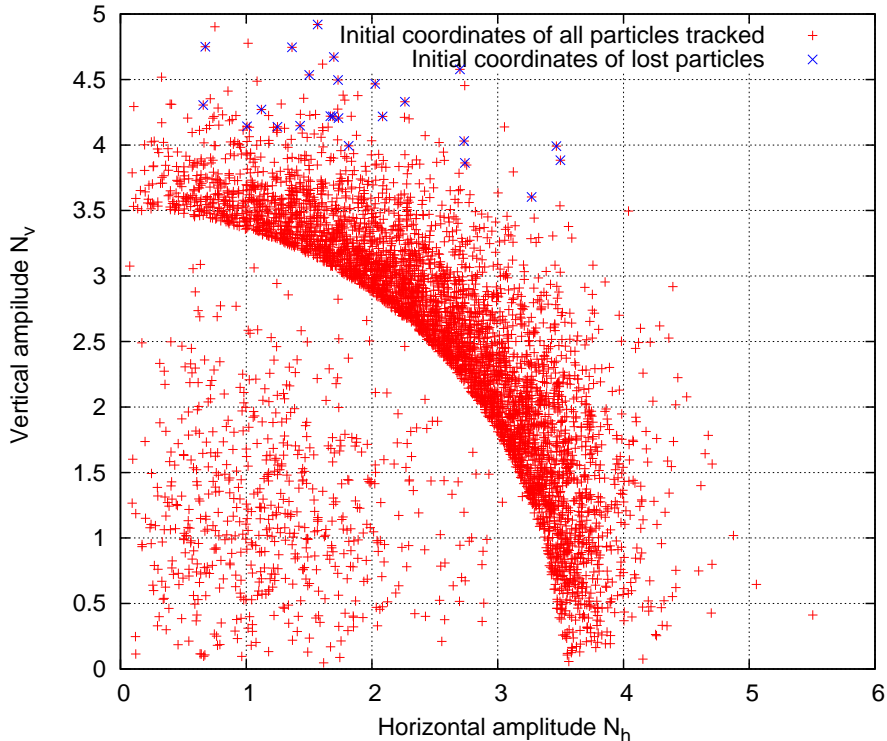


Figure 3: Initial coordinates of all tracked particles and of the lost particles.

Knowing the ratio between the to-be-tracked particle number (here it is 4800) and the total particle numbers in the Gaussian distribution, we are able to determine the percentage of lost particles in a real 6-D Gaussian distribution from the number of lost particles in the hollow Gaussian distribution. As discussed, the particles below the transverse and longitudinal tracking boundaries are assumed to be stable and will not be tracked.

The last step to generate the initial particle coordinates is to convert the normalized coordinates  $(x_n, p_{xn}, y_n, p_{yn})$  to the real space coordinates  $(x, p_x, y, p_y)$ . In the particle tracking, we use  $(x, p_x, y, p_y, z, \delta)$ .

## 2.5 One example

Here we give an example to show the tracking with a hollow Gaussian bunch. Figure 3 shows the initial transverse coordinates of particles in a 6-D hollow Gaussian distribution. The tracking condition are: proton bunch intensity  $N_p = 2.5 \times 10^{11}$  with half head-on beam-beam compensation. The boundaries of the hollow Gaussian distribution are  $3.5\sigma$ . Particles with relative transverse amplitude larger than  $3.5\sigma$  or with relative longitudinal amplitude larger than  $3.5\sigma$  are to be tracked. The total number of particles are to be tracked is 4800 which represent a 6-D Gaussian bunch with a population of 266947. From Figure 3, there are particles below transverse amplitude  $3\sigma$ . These particles are to be tracked because their relative longitudinal amplitude is larger than  $3.5\sigma$ .

Figure 3 also shows the initial coordinates of lost particles in the  $2 \times 10^6$  turn tracking. From Figure 3, the lost particles are well above the transverse tracking boundary  $3.5\sigma$  and there is no single particle lost below transverse tracking boundary  $3.5\sigma$  regardless their initial relative longitudinal amplitudes larger than  $3.5$ . Also from Figure 3, the initial coordinates of lost particles are mostly near  $75^\circ$  in the x-y plane, which is consistent with previous dynamic aperture calculation.

Since there is a spread in the initial transverse amplitude of the lost particles, to better reflect the particle loss in a real bunch, we should use caution to choose a boundary below which the particles are assumed to be stable. If the boundary is chosen too low, there will be few particles lost in the tracking and the statistic error in the calculate particle loss percentage will be large. If the boundary is chosen too high, there will be lost particles whose initial coordinates are on or close to the boundary. In this case the particle loss will be under estimated. And if the boundary is chosen larger than  $4\sigma$ , we may need to use a special Gaussian tail generator.



### 3 Tracking results

#### 3.1 Without beam-beam compensation

Figure 4 shows the normalized beam intensity without and with half beam-beam compensation for three proton bunch intensities  $2.0 \times 10^{11}$ ,  $2.5 \times 10^{11}$  and  $3.0 \times 10^{11}$ . From Figure 4, in the  $2 \times 10^6$  turn tracking, half beam-beam compensation reduces proton particle loss for bunch intensities  $2.5 \times 10^{11}$  and  $3.0 \times 10^{11}$ . However, for bunch intensity  $2.0 \times 10^{11}$  half beam-beam compensation increases the proton particle loss.

#### 3.2 With multiple $\pi$ phase advances between IP8 and e-lens

For half head-on beam-beam compensation, to better compensate the nonlinearities from the proton-proton beam-beam interaction at IP8 with the e-lens around IP10, we will adjust the betatron phase advances between IP8 and the center of e-lens to be multiples of  $\pi$ . Without any beam-beam interaction and phase adjustment, the betatron phase advances between IP8 and the center of the e-lens are  $(8.5\pi, 11.1\pi)$ . In this study, we will adjust the betatron phase advances between IP8 and the center of e-lens to be  $(7\pi, 9\pi)$ .

To adjust the phase advances between IP8 and e-lens, we insert two artificial betatron phase shift matrices before and after e-lens in the lattice model. The phase shift matrices don't change the overall ring tunes and Twiss parameters. However, the exact  $(7\pi, 9\pi)$  betatron phase advances are only given for on-momentum particles because of the chromatic tune shift.

Figure 5 shows the relative beam intensity with phase advances of  $k\pi$  between IP8 and e-lens in presence of half head-on beam-beam compensation. From Figure 5, phase adjustment does reduce the proton particle loss rates for the three bunch intensities. For bunch intensities  $2.5 \times 10^{11}$  and  $3.0 \times 10^{11}$ , the multipole  $\pi$  phase advances reduce the beam loss to half of that without head-on beam-beam compensation.

#### 3.3 Scan of first order chromaticity

We scan the first order chromaticity  $Q'$  with half head-on beam-beam compensation and the phase advances of  $k\pi$  between IP8 and the e-lens. By adjusting first order chromaticities with chromatic sextupoles in the arcs, the off-momentum phase advances between IP8 and e-lens will be adjusted too. In this study we choose the proton bunch intensity  $2.5 \times 10^{11}$ .

Figure 6 shows the relative proton beam intensity with different first order chromaticity in the presence of half head-on beam-beam compensation. The phase advances of  $k\pi$  between IP8 and the e-lens are included. In this scan, the horizontal and vertical first order chromaticities are always set equal.

From Figure 6, zero chromaticity gives the best beam lifetime. When the chromaticity is increased from 0 to 4, the proton lifetime drops. For a linear chromaticity with +3, comparing to that with zero linear chromaticity, the beam lifetime drops by a factor of 6 in the  $2 \times 10^6$  turn tracking.

#### 3.4 With second order chromaticity correction

Here we study the effect of second order chromaticities  $Q''$  on the particle loss in the presence of half head-on beam-beam compensation. With second order chromaticity correction, the chromatic betatron tune spread will be smaller. In the simulation, we used the convenient 4 knobs suggested in Ref. [9] to minimize the second order chromaticities. The second order chromaticities in horizontal and vertical planes are about (2400, 2700) before correction, and are below 500 after correction.

Figure 7 shows the normalized proton beam intensity without and with second order chromaticity correction. Betatron phase advances of  $k\pi$  between IP8 and e-lens are included. The first order chromaticities are set to +1. From Figure 7, the second order chromaticity correction does reduce the proton particle loss rate, especially for bunch intensities  $2.0 \times 10^{11}$  and  $2.5 \times 10^{11}$ . For bunch intensity  $3.0 \times 10^{11}$ , the improvement is smaller.

#### 3.5 Scan of the proton working point

Here we scan the working point of the proton beam. In the above studies, the proton beam working point is set to (28.67, 29.68) with beam-beam and its compensation. Due to the limited tune space between  $2/3$  and  $7/10$ , we only can scan several working points along the diagonal. In this study the difference in the transverse fractional tunes is set to 0.005. The tunes are with beam-beam and its half compensation.

Figure 8 shows the relative proton beam intensity in the tune scan. Half beam-beam compensation together with multiple  $\pi$  phases advances between IP8 and e-lens and second order chromaticity correction are included. The proton bunch intensity in this study is  $2.5 \times 10^{11}$ .

From Figure 8, the working points (28.675, 29.67) and (28.67, 29.675) give best proton beam lifetime in the presence of half beam-beam compensation, while the working points (28.685, 29.68) and (28.68, 29.685) give worst beam lifetime. Also from Figure 8, normally the proton beam lifetime is better with a working point below the diagonal than that with the horizontal and vertical swapped working point above diagonal.

### 3.6 Scan of the electron beam intensity

Here we scan the electron beam intensity in the head-on beam-beam compensation. We calculated the cases with the proton-proton beam-beam parameter compensated by factor of 1/4, 1/2 (half), 3/4 and 1.0 (full). For example, for 1/4 beam-beam compensation, a quarter of the total proton-proton beam-beam parameter will be compensated. In the study, the tunes are always set to (28.67, 29.68) with the beam-beam interaction and its compensation. And the phases advances of  $k\pi$  between IP8 and e-lens and second order chromaticity correction are included. The proton bunch intensity is  $2.5 \times 10^{11}$ .

Figure 9 shows the normalized proton bunch intensity with different fractional head-on beam-beam compensation. In the Figure 9, the curves of 3/4 and full beam-beam compensation are missing since the huge proton loss in these cases are out of the vertical axis range. For 3/4 and full beam-beam compensation, the relative proton intensity after  $2 \times 10^6$  turns are about 0.9995 and 0.9965 respectively, which are worse than that without beam-beam compensation.

From Figure 9, for proton bunch intensity  $2.5 \times 10^{11}$  in the  $2 \times 10^6$  turn, half head-on beam-beam compensation gives better proton lifetime than that without compensation and with only a quarter compensation. A quarter head-on beam-beam compensation is not enough for the bunch intensity  $2.5 \times 10^{11}$ .

### 3.7 Scan of the electron beam size

In the above simulation, the electron beam always has the same transverse beam size as the proton beam in the e-lens. Here we slightly adjust the electron beam proton to check its effect on the proton lifetime time. In the study, bunch intensity is  $2.5 \times 10^{11}$  and the phases advances of  $k\pi$  between IP8 and e-lens and second order chromaticity correction are included. The working points with beam-beam and half compensation are set to (28.67, 29.68).

Figure 10 shows the relative proton beam intensity with different electron beam size. From Figure 10, for proton bunch intensity  $2.5 \times 10^{11}$  in the  $2 \times 10^6$  turn tracking, the electron beam size with 20% and 40% larger than the proton's gives better proton beam lifetime. The electron bunch size with 20% smaller than the proton's gives a lot particle loss and is out of the vertical range in Figure 10. The relative proton beam intensity with 20% smaller electron beam size is about 0.9988. This study shows that the proton beam with bunch intensity  $2.5 \times 10^{11}$  does prefer a larger electron beam size in the half head-on beam-beam compensation.

### 3.8 Scan of the transverse offset of electron and proton beams

Here we check the effect of the transverse offset of the electron and proton beam in the e-lens in the presence of half head-on beam-beam compensation. In the above study, the electron beam and proton beam are centered on the beam pipe axis. In the study, we will shift the electron beam from the center of beam pipe. The electron beam has the same transverse beam size as the proton beam in the e-lens.

Figure 11 shows the closed orbit of proton beam due to transverse offset of the electron beam in the e-lens. In this calculation the transverse offset of the electron beam is assumed be  $1.5\sigma$  of the proton beam size. Figure 12 shows the closed orbit of the proton beam at IP6, IP8 and in the e-lens as function of the transverse offset of the electron beam in the e-lens. From Figure 12, With transverse offset of the electron beam in the e-lens will offset the proton-proton beam-beam collisions at IP6 and IP8. The maximum perturbation to the proton closed orbit is with electron transverse offset about  $1.5\sigma$ . The maximum offset of proton-proton collisions at IP6 and IP8 is about 5 6% of proton beam size there.

Figure 13 shows shows the relative proton beam intensity with the electron beam offset. The offset of the proton-proton collisions at IP6 and IP8 are corrected. From Figure 11, comparing to the zero offset, there is a clear proton lifetime drop with more that one proton beam size offset of electron beam. In the real operation, we should steer the proton beams at IP6 and IP8 to exact head-on collisions.

### 3.9 Scan of the random noise in the electron density

Here we study the effect of random noise in the electron bunch intensity onto the proton beam lifetime in the presence of half head-on beam-beam compensation. We define the percentage noise amplitude  $|dI/I_0|$  as the maximum amplitude of the random noise divided by the nominal electron beam intensity. In the study, we adopt a proton bunch intensity  $2.5 \times 10^{11}$  and the phases advances of  $k\pi$  between IP8 and e-lens and second order chromaticity correction are included.

Figure 12 shows the relative proton beam intensity with random noise in the electron beam intensity. From Figure 12, for bunch intensity  $2.5 \times 10^{11}$ , below 0.1% random noise in the electron beam is acceptable in the  $2 \times 10^6$  turn tracking. The fluctuation in the electron beam intensity is determined by the stability of the involved power supplies of the electron gun.

## 4 Summary

In this note we calculated and compared the particle loss in a proton bunch in presence of head-on beam-beam compensation. The Blue ring 250 GeV proton run lattice with  $\beta^* = 0.5$  m is used. Three bunch intensities  $2.0 \times 10^{11}$ ,  $2.5 \times 10^{11}$  and  $3.0 \times 10^{11}$  are chosen although in most parameter scans we used bunch intensity  $2.5 \times 10^{11}$ . To save computing time and to overcome large statistic fluctuations in the particle loss calculation, we tracked particles with a 6-D hollow Gaussian distribution. The 6-D synchro-beam map a la Hirata is used for the proton-proton beam-beam interaction simulation at IP6 and IP8. The e-lens is modeled as 8 slices and each slice is modeled with drift-4D beam-beam kick-drift.

From the particle trackings up to  $2 \times 10^6$  turns, we found that half head-on beam-beam compensation greatly reduces the particle loss with bunch intensities  $2.5 \times 10^{11}$  and  $3.0 \times 10^{11}$ . The betatron phase advances of  $k\pi$  between IP8 and the e-lens and the second order chromaticity correction further increase the proton beam lifetime in the presence of half head-on beam-beam compensation.

We also found that full head-on beam-beam compensation introduces too much nonlinearity into the proton beam dynamics and therefore reduces the lifetime of proton beam. Half head-on beam-beam compensation is the optimum for a proton bunch intensity  $2.5 \times 10^{11}$ . We scanned the first order chromaticity and working point of the proton beam in the presence of half beam-beam compensation for bunch intensity  $2.5 \times 10^{11}$ . We found from simulation that slightly larger transverse electron beam size than that of proton beam in the e-lens gives a larger proton lifetime with half beam-beam compensation and the random noise in the electron density less than 0.1% is safe to the proton lifetime.

In all our simulations, the beam losses are substantially smaller than that in the machine operation. Efforts are under way to calibrate the simulations better with the measurements.

All the simulations in the article were done with SimTrack [10]. SimTrack is a c++ library for optical calculation and particle tracking in high energy circular accelerators.

## 5 Acknowledgment

The authors would like thank Y.-J. Kim (FNAL) to help implement 6-D weak-strong beam-beam in the SimTrack. We also thank Y.-J. Kim, A. Valishev (FNAL) and M. Blaskiewicz, X-F. Gu and C. Montag for fruitful discussions during this study.

## References

- [1] V. Shiltsev, *Electron lenses in Tevatron, RHIC and LHC*, in the 2005 RHIC APEX workshop, BNL, November 2005.
- [2] Y. Luo and W. Fischer, *Outline of using an electron lens for the RHIC head-on beam-beam compensation*, BNL C-AD AP Note 286, July 2007.
- [3] C. Montag, private communications, 2010.
- [4] K. Hirata, H. Moshhammer, F. Ruggiero, A symplectic beam-beam interaction with energy change, Particle Accel. 40 (1993) 205-228.

- [5] M. Bassetti and G.A. Erskine, *Closed expression for the electrical field of a two-dimensional Gaussian charge*, CERN-ISR-TH/80-06.
- [6] R.D. Ruth, "A canonical Integration Technique", IEEE Trans. Nucl. Sci., vol. NS-30, PP.2669-2671 (1983).
- [7] GNU Scientific Library, <http://www.gnu.org/software/gsl/>.
- [8] Y. Luo and W. Fischer, *Simulation study of dynamic aperture with head-on beam-beam compensation in the RHIC*, BNL C-AD AP Note ???, April, 2010.
- [9] Y. Luo, et al., *Sorting chromatic sextupoles for easily and effectively correcting second order chromaticity in the Relativistic Heavy Ion Collider*, BNL C-A/AP/348, January, 2009.
- [10] Y. Luo, *SimTrack User's Manual ( v1.0 )*, BNL C-AD AP Note 388, January, 2010.

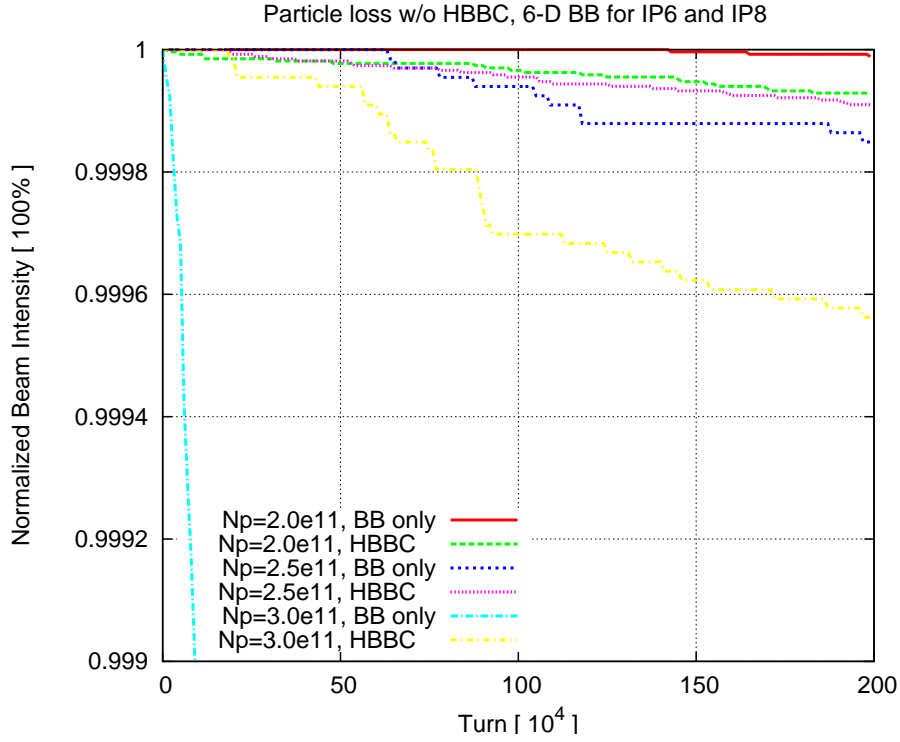


Figure 4: Particle loss without and with half head-on beam-beam compensation.

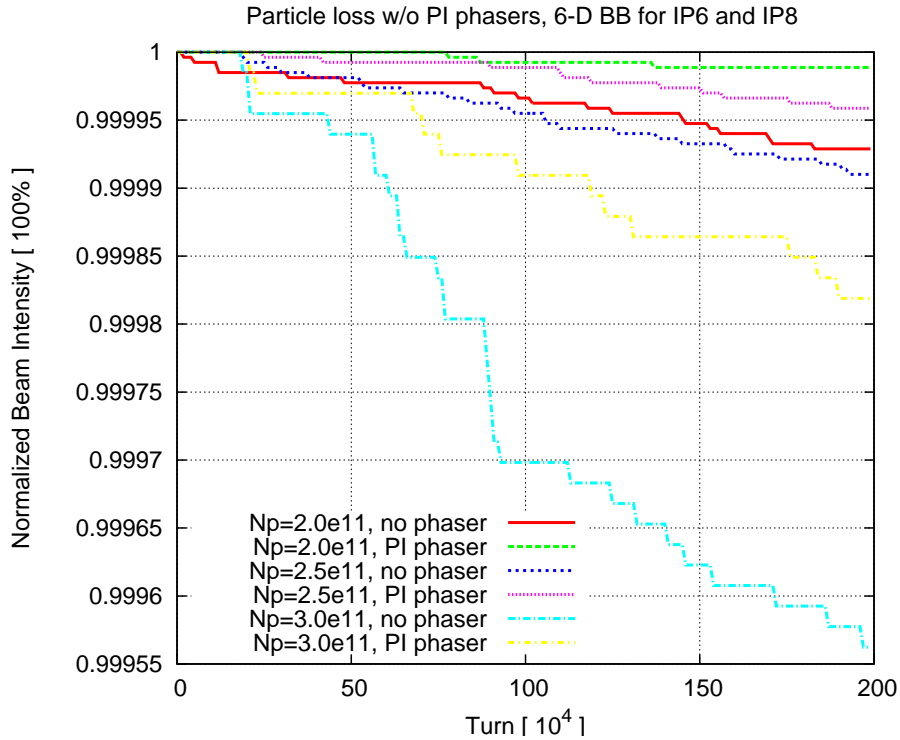


Figure 5: Particle loss without and with multiple  $\pi$  phase advances between IP8 and e-lens.

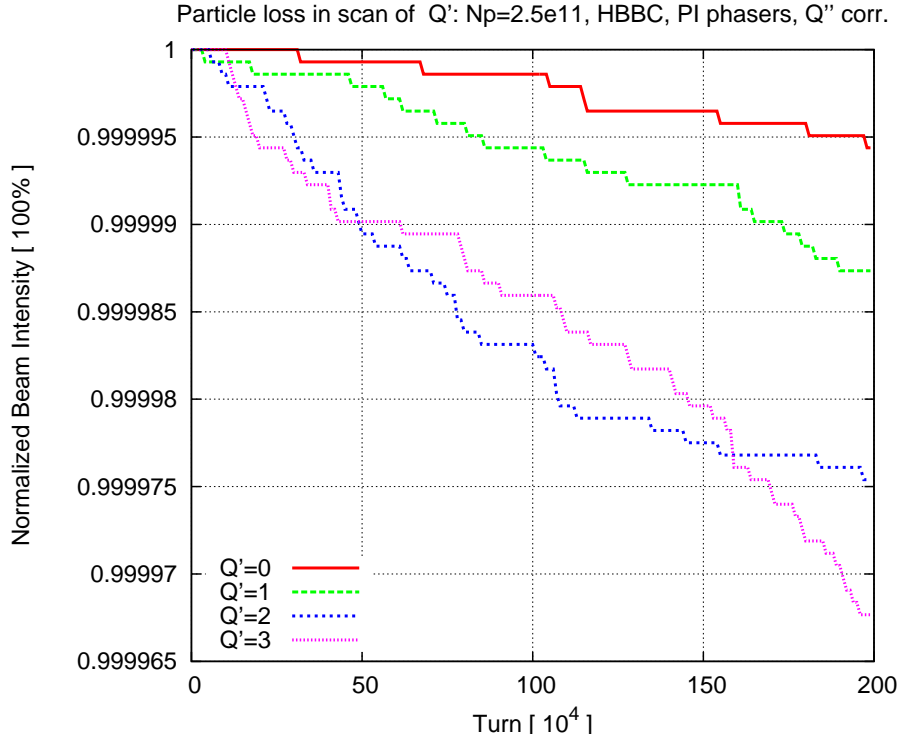


Figure 6: Particle loss with half head-on beam-beam compensation in the scan of first order chromaticity.

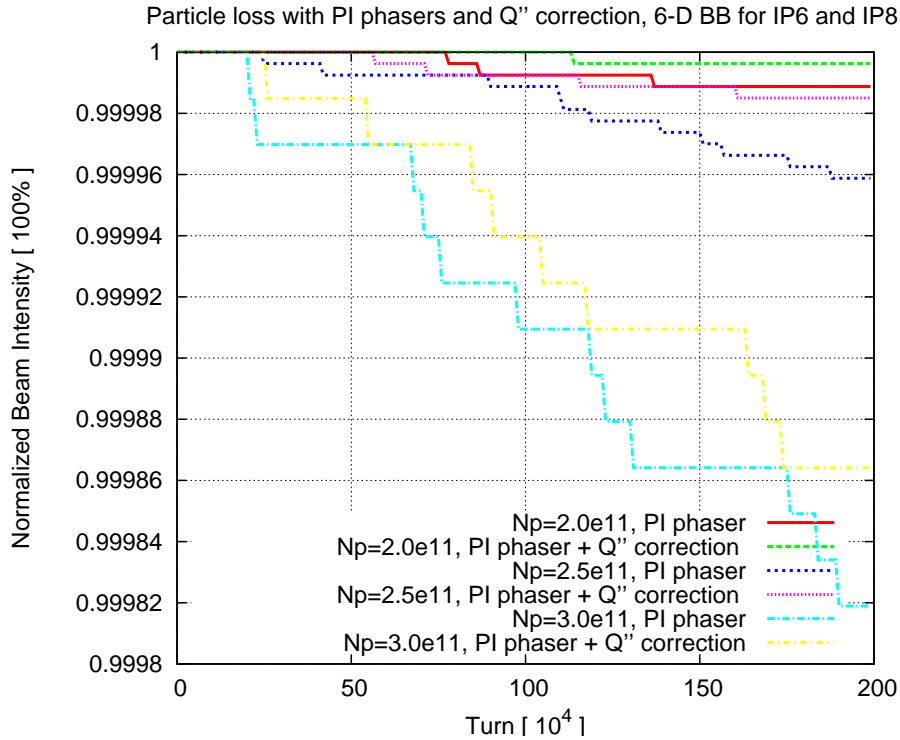


Figure 7: Particle loss without and with second order chromaticity correction.

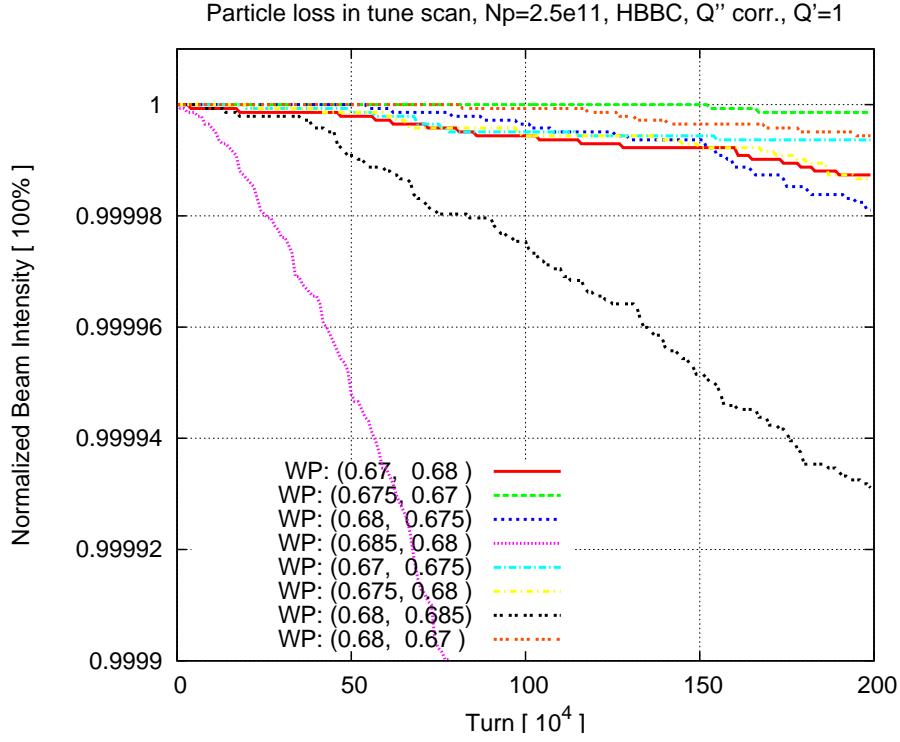


Figure 8: Particle loss with half head-on beam-beam compensation in the scan of proton working point.

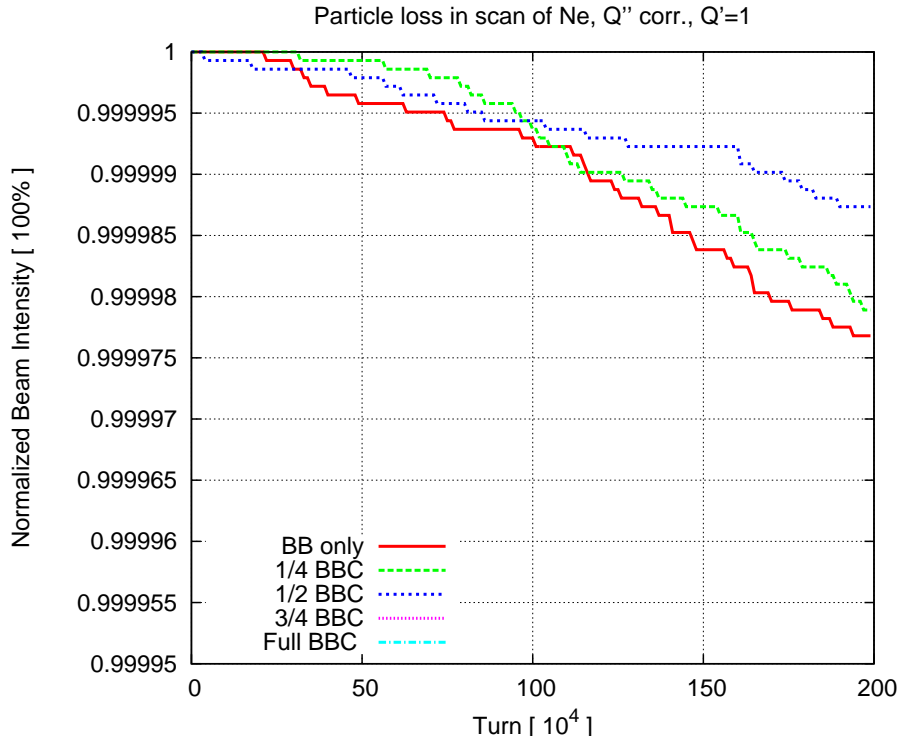


Figure 9: Particle loss 1/4, 1/2 (half), 3/4 and 1.0 (full) head-on beam-beam compensation.

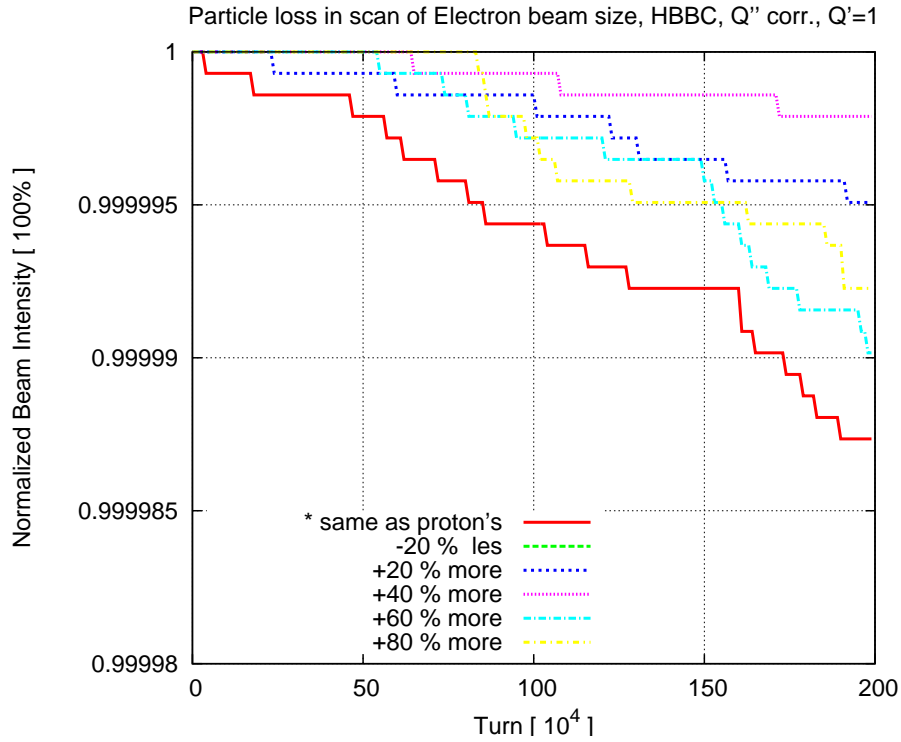


Figure 10: Particle loss with half head-on beam-beam compensation in the scan of electron transverse beam size.

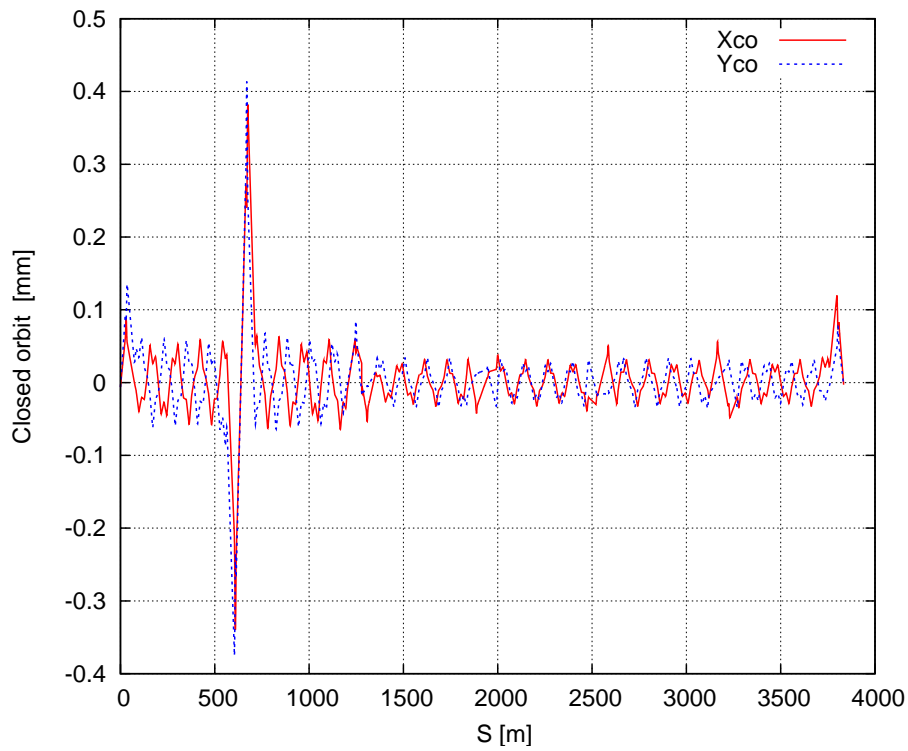


Figure 11: Closed orbit along the ring introduced by the transverse offset of electron beam. In this example, the electron beam is 1.5 proton beam size off set.



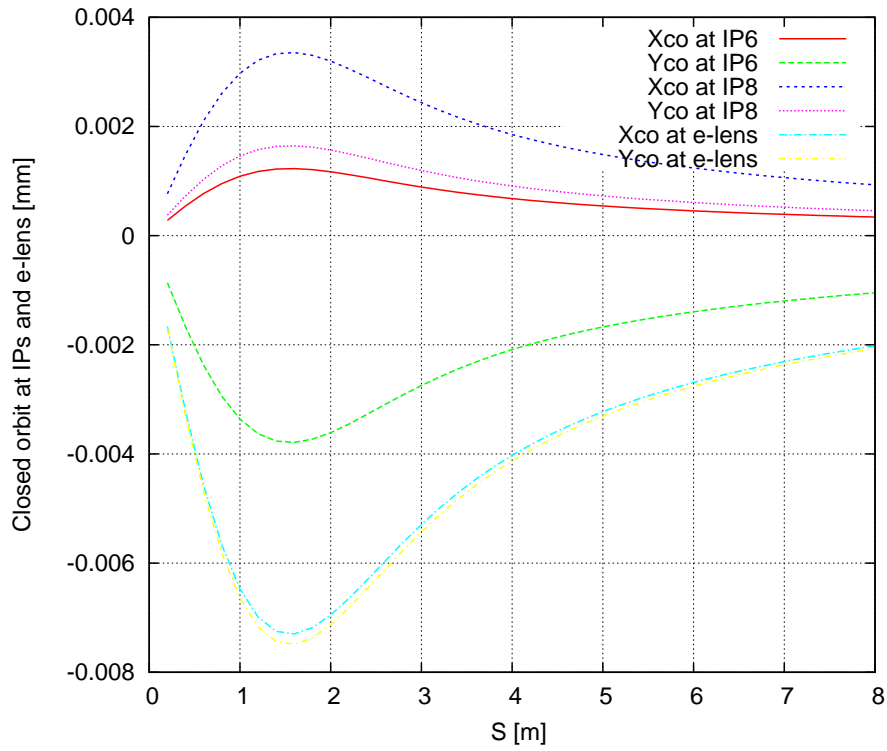


Figure 12: The closed orbit at IPs and e-lens as function of the transverse offset of electron beam.

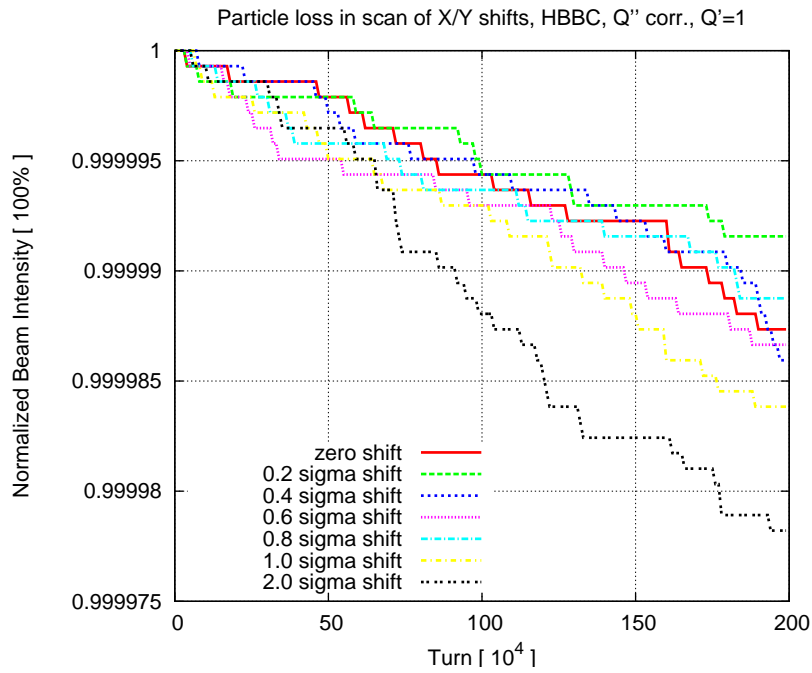


Figure 13: Particle loss with transverse electron beam offset in the e-lens.

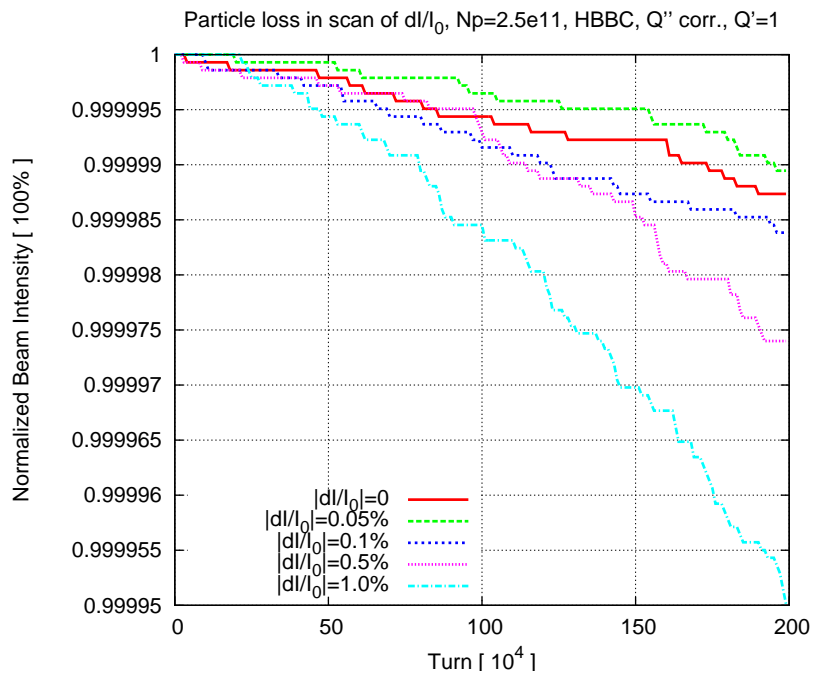


Figure 14: Particle loss Layout of RHIC head-on beam-beam compensation.